203. Static model tests on long-span twin-fan-shaped space frames for retractable roofs

A. HORI, Hazama Corporation, Japan, A. WADA, Tokyo Institute of Technology, Japan, and Y. MAKINO, Kumamoto University, Japan

SYNOPSIS. Static loading tests on 1/100 scale models of a raised double-layered space truss of complicated-shape have been carried out. The truss has a twin-fan-shaped plan form, because it was designed as one of four retractable roofs to cover a circular space. Members were modelled as 5.0-2.0mm diameter copper pipes. Two specimens were tested under either asymmetrical vertical load or span-directional horizontal load. The main conclusions are that buckling length of a chord in a rigid jointed truss can be evaluated as that of two continuous chords, and that the macro-behaviour of these complicated trusses may be explained by a simple model.

INTRODUCTION

1. Many long-span structures have been erected in recent years, and the double-layered and raised space truss is a very effective form for spans of 100-200m. Experimental studies on double-layered space trusses have been reported by Schmidt (ref. 1), Collins (ref. 2) and many other researchers. However for the raised case, very few tests have been carried out. This paper reports on the elasto-plastic static loading tests on 1/100 scale models of a raised double-layered space truss of complex shape, which is designed for one of the retractable roofs in a proposed domed stadium (ref. 3). Specimens have a twin-fan-shaped plan form and one longitudinal general arch in each. The number of members and of translational freedoms in a specimen is about 2190 and 1890, respectively. Two specimens were examined under either asymmetrical vertical load or span-transverse horizontal uniform load.

SPECIMENS

2. Shape of specimens. Overall dimensions of the 1/100 scale specimens are shown in Fig. 1. They have a 2200mm length, about 850mm width and 450mm height, 32.5mm depth and a rise-span ratio of approximately 0.20. Fig. 2 shows the framed shape of the specimens. It consists of main-trusses (left half of Fig. 2 (a)), which contain two lower chords and one upper chord in each, and secondary members (right half of the figure). The number of main-trusses decreases toward

Space structures 4. Thomas Telford, London, 1993

the top. Plans of upper chords, lower chords and diagonals are shown in the left half of Fig. 2(b)-(d), respectively. Diagonals between main-trusses are located basically at intervals of one row.

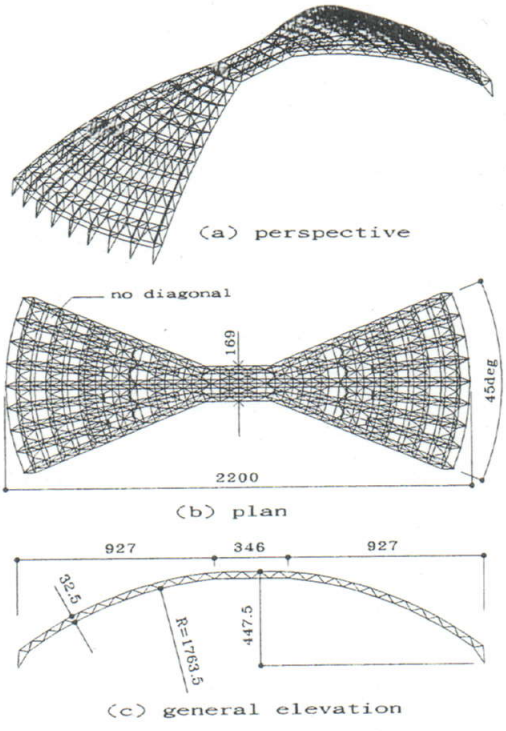

Fig. 1. Overall dimensions of specimen.

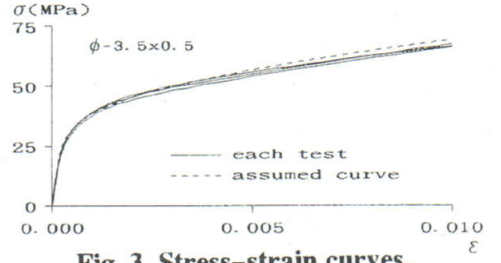

Fig. 3. Stress–strain curves.

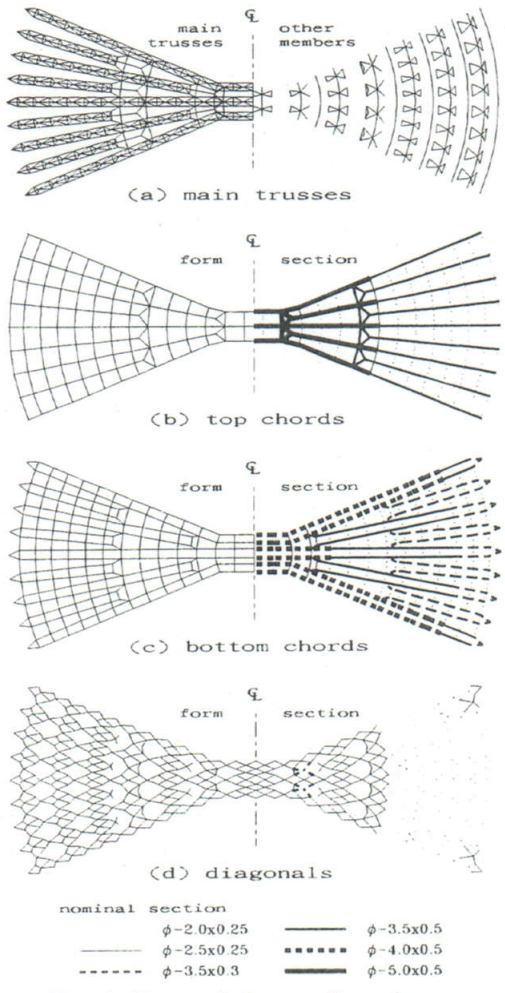

Fig. 2. Framed shape of specimen.

Table 1. Properties of sections and material test results.

nominal section	D (mm)	A (mm²)	t (mm)	r (mm)	E (MPa)	$\sigma_{0.2}$ (MPa)	σ_{max} (MPa)	ε_{max} (%)
φ-5.0x0.5	4.97	6.82	.484	1.60	125000	47.5	229	56
φ-4.0x0.5	3.97	5.47	.502	1.24	130000	49.3	231	53
φ-3.5x0.5	3.46	4.44	.473	1.07	127000	47.2	230	51
φ-3.5x0.3	3.48	2.70	.268	1.14	120000	58.4	232	–
φ-2.5x0.25	2.48	1.57	.221	0.802	112000	44.0	>217	–
φ-2.0x0.25	1.97	1.30	.238	0.617	117000	56.3	241	44

D: diameter A: area t: thickness (calculated from D and A)
r: radius of gyration E: young modulas $\sigma_{0.2}$: 0.2% offset strength
σ_{max}: maximum strength ε_{max}: elongation

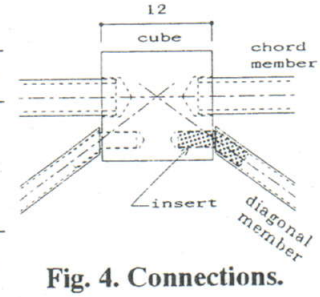

Fig. 4. Connections.

3. Members. Ready-made copper pipes were annealed and used for member Sections were selected among the six sizes shown in Table 1, to maintain th original slenderness ratio between nodes as closely as possible. The size of eac member is shown in the right half of Figs 2(b)-(d) for upper chords, lowe chords and diagonals, respectively. Their sizes increase toward the top. Materi test results of the annealed pipes are shown in the right hand columns of Table and the stress-strain curve is shown in Fig. 3. Offset strength at 0.2% is 4 58MPa and hardening is greater than for structural steel.

4. Fabrications. Connections were replaced by 12mm regular cubes of coppe Most of the chord ends were brazed into machine-made holes in the cubes. Detai are shown in Fig. 4. All diagonals and the rest of the chords, which joi obliquely to cube-faces, are brazed through L-shaped-inserts as shown in Fig. The support condition at the specimen base is fixed. The total weight of on specimen is about 12kg. The members were located and assembled on a twin-fan shaped steel having high accuracy, bolting most of the cubes.

BUCKLING STRENGTH OF CHORDS

5. Chord tests. Axial force-displacement relations for single chords wer examined for each section. Chord specimens have 86.5mm length for th standard lower chord and pinned ends (Fig. 5). Test results are shown by th solid line in Fig. 5. The strength of each section at first buckling exceeds th 0.2% offset value. The broken line in the figure shows the axial force calculate from experimental strains at the specimen centre, where damage is most concentrated. For this calculation, a stress-strain model is extended from th Ramberg-Osgood Model as shown in Fig. 6. Furthermore, constant volume i assumed and stress is multiplied by 1/(1+strain). The calculated force (broken lin in Fig. 5) agrees very well with the experimental results. Therefore, the axia force of the member is well-approximated from the elasto-plastic experimenta strains under an appropriate stress-strain assumption.

6. Analysis. Results of a buckling analysis using fibres with the stress-strai model of Fig. 6 are shown by the dotted line in Fig. 5. It agrees well with th experimental results.

7. Buckling forms and strength. Ignoring rotational constraint by diagonals a chord ends, chord buckling can be modelled as 1:pinned-pinned, 2:tripled 3:pinned-fixed or 4:fixed-fixed, as shown in Fig. 7(a). However, the differenc between 2 and 3 above turns out to be small on the analytical axial force displacement curves under monotonic compression for all section sizes Therefore, by adding diagonals as rotational elasto-plastic spring at the chor ends, two further models were analysed, 5:springed-springed and 6:springed fixed. Their axial force-displacement curves are shown by the solid and roughly broken lines in Fig. 7(b), respectively. Buckling strength is significantly increased by rotational constraint of diagonals.

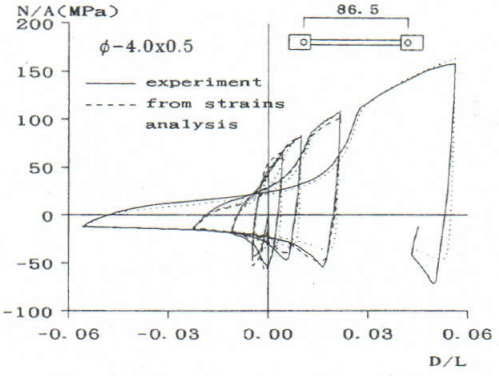

Fig. 5. Chord tests and analysis.

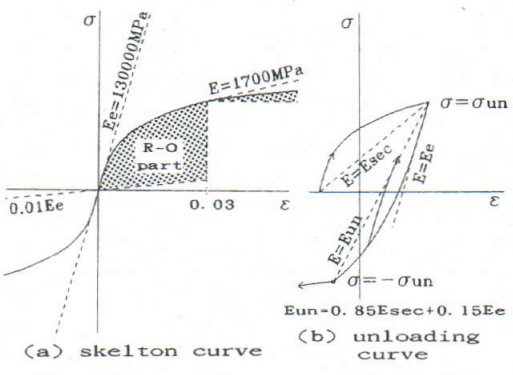

Fig. 6. Extended stress–strain model.

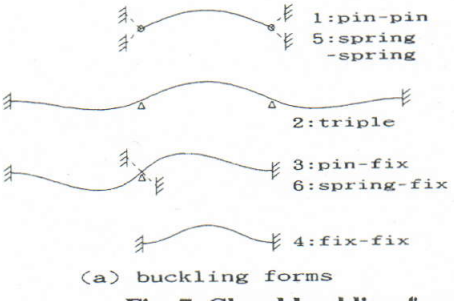

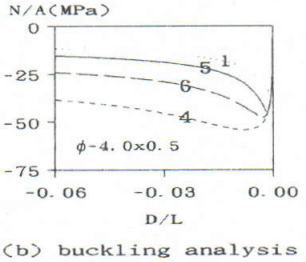

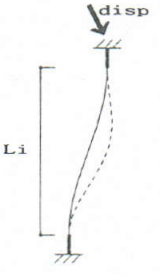

Fig. 7. Chord buckling forms and analysis.

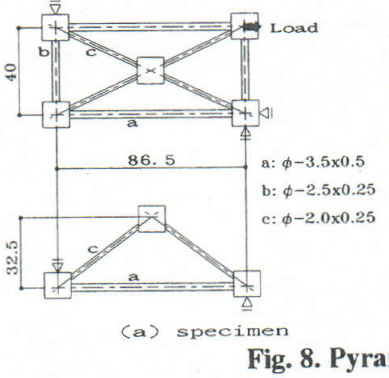

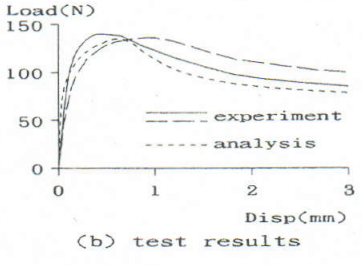

Fig. 8. Pyramid tests.

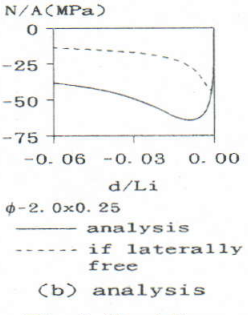

Fig. 9. Buckling of diagonals.

BUCKLING STRENGTH OF DIAGONALS

8. Pyramid tests. The buckling strength of diagonals was examined by pyram specimens (Fig. 8(a)) which correspond to one of the typical parts of the twi fan-shaped specimen. Three specimens are loaded monotonically at one of t cubes in a pyramidal base, to put two opposite diagonals in compression and t others in tension. Load-displacement curves are shown in Fig. 8(b). The sol and broken lines correspond to typical and another type whose buckling wav are observed at one or two diagonals, respectively. Plastic hinges due to buckli formed at the inner ends of the L-shaped -inserts.

9. Forms and strength of diagonals. If both ends of the buckled diagonals a fixed rotationally and changes of other member lengths are small, buckling modelled under relative translational displacement, which is oblique to t member axis as shown in Fig. 9(a). However, their analytical axial forc displacement curves are the same as the non-oblique results (one solid line in Fi 9(b) shows both results). Therefore, diagonal buckling can be evaluated as if bo ends are fully fixed. The load-displacement curve of the pyramid is calculat using the analytical curve of a diagonal, and shown by the dotted line in Fi 8(b). It agrees well with typical experimental results.

ASYMMETRICAL VERTICAL LOAD TEST

10. Earthquake and wind loads are severe in some countries. Longitudin earthquake excitation to an arch causes asymmetrical vertical inertia forces, whi were severe in this design (ref. 3), because horizontal displacement at the arch t brings vertical displacement anti-symmetrically to the right and left halves.

11. Loading and measurements. A twin-fan-shaped specimen was tested und simplified asymmetrical load that is a downward load on half of its arch. Usi the tournament method, 28 cubes on the lower chord surface of a half side we pulled proportionally to the dead load in design. Fig. 10(a) shows t tournament, which has a loading screw as well as a load-cell. Centripet displacements of the spherical-shell-like specimen were measured at 22 cub shown by blacked circles in Fig. 10(b). Horizontal values were measured at cubes shown by arrows indicating their directions. Strains were measured with strain-gauges for each section at the centres of 47 members, shown by bold lin in the figure.

12. Progress. Fig. 11(a) shows heavy or moderate damage after testin Damage progress is as follows. (a) No damage is observed before the maximu strength. (b) After strength falls slightly, continued buckling of two or thr chords is observed at mid-height in the loaded half. (c) Diagonals adjacent to t buckled chords are clearly bent. Chord buckling is newly observed at upper a middle height in the other half, and damage of chords and diagonals is observ just above both bases. This state means that four or more macroscopic hing form along the overall arch, leading to macroscopic instability. Strength at t time is 90% of the maximum. (d) Buckling and damage becomes heavier and t test finishes after the maximum displacement reaches 5% of the span. The to number of damaged members was up to 12% of the total. Typical buckling of t

upper chord is out-of-plane as shown in Photo 1(a), though some buckled in-plane (Photo 1(b)).

13. Results. Relations of load and centripetal displacements are shown in Fig. 12. The maximum strength is 839N. These curves display very smooth shapes, slow strength reduction and asymmetrical deformation of the arch, which is convex downward at the loaded half and upward at the other half. In the arch-transverse direction, centripetal displacements are almost the same and show no remarkable asymmetrical deformation. Bending moment of the centre main-truss calculated from the chord strains is shown in Fig. 13. Bending strength at the most damaged part decreases in the final state.

14. Maximum strength by simple analysis. Modelling a specimen as a planer pinned truss as shown in Fig. 11(b), maximum strength is calculated using the springed-fixed strength of §7. Analytical buckled members are shown in the figure and the overall strength is 92% of the experimental value. These indicate good agreement with experimental results. Therefore, strength and macroscopic damage are also well estimated by a simple model which simulates the collapse mechanism well, as long as the member strength is properly evaluated.

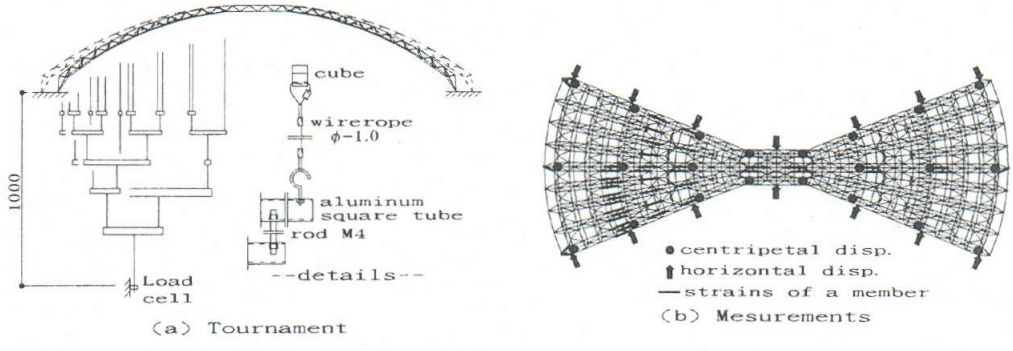

Fig. 10. Loading and measurements of asymmetrical vertical load test.

15. Considerations. The above results are summarised as follows for buckling length: (a) Buckling of continuous chords occurred first. (b) The number of buckling continuation was equal or less than 3, because of the gradient of the axial force. (c) The strength of three continuous chords is nearly equal to that of two. (d) The overall strength is explained by member strength of two chords with rotational constraint by diagonals. From (a)-(d) above, the buckling length of a chord in a rigidly-jointed truss can be evaluated as that of two continuous chords, if preceded by elasto-plastic chord buckling. Ignoring rotational constraint in the case of two equalised chords, it is simplified as 0.7 times their nodal length.

TRANSVERSE HORIZONTAL LOAD TEST

16. A specimen was tested cyclically under span-transverse horizontal load, which is the most severe in this design and makes the behaviour more complicated. Because distribution of the maximum inertia force of the earthquake response analysis in the design was approximately uniform span-directionally, the experimental distribution is also set to be uniform.

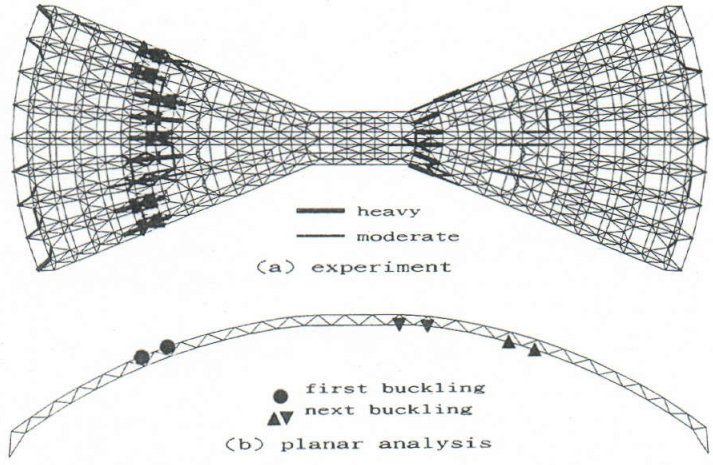

Fig. 11. Damage of asymmetrical vertical load test.

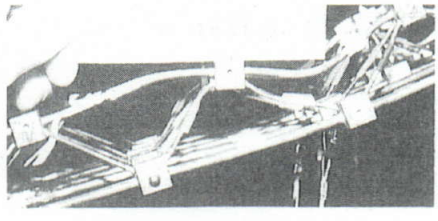

(a) typical one

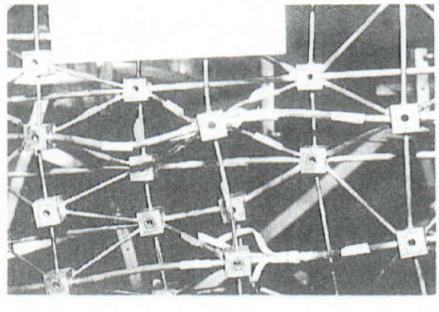

(b) fewer type

Photo 1. Buckled upper chords.

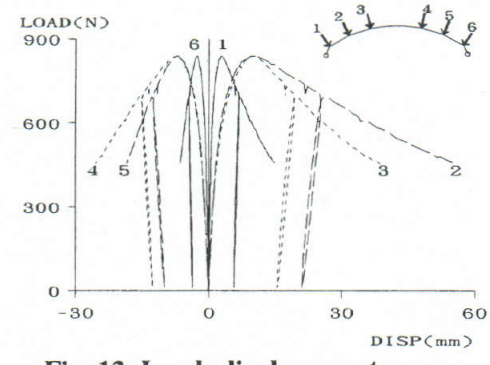

Fig. 12. Load–displacement curves.

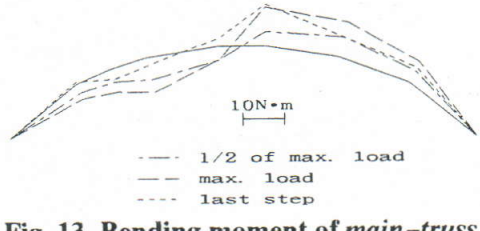

Fig. 13. Bending moment of *main–truss*.

17. Loading and measurements. Fig. 14(a) shows a plan of the tournaments. One tournament is used for loading and the other is used as a counter-weight. The total load is distributed to 16 cubes on the front surface of the specimen. A view of the test is shown in Photo 2. Cyclic loading is controlled by top displacement divided by span with a target of plus-minus 1/1000, 1/500, 1/200 or 1/100, for 1st-4th cycles, respectively. Final loading is carried positive. Centripetal displacements are measured at 22 cubes shown by blacked circles in Fig. 14(b) and horizontal displacements at 22 cubes shown by arrows. Strains are measured at 49 members shown by bold lines in the figure.

18. Progress. Fig. 15 shows major damage at positive cycles and that near the top at final loading. Damage progress is as follows: (a) No damage is observed in the first two cycles. (b) Buckling of diagonals is observed at 1/200 cycle in most of the 16 pyramidal portions, which are between main-trusses and just above the bases. They are considered as a result of the in-plane shear like pyramid-tests. Damage is also observed at lower chords on both bases in the front half of loading direction. (c) They spread to above the bases and to the other half at 1/100 cycles. Upper chords are damaged in the other half above the bases. Photo 3(a) shows a view around a base. (d) The above damage becomes heavier, and overall sinking is observed at final loading. Eventually, slight strength reduction is caused with upper and lower chord buckling near the top. Photo 3(b) shows an overall final view. The number of damaged members was up to 17% of the total.

19. Results. The load vs. top displacement curve is shown in Fig. 16. The maximum strength up to 1/200 cycle is plus 1160N and minus 1190N, values almost the same as the overall maximum. Strength reduction after diagonal buckling is not clear, and the shape of hysteresis loops is energy-dissipative. Overall deformed shape after test is shown by the broken line in Fig. 17, with the

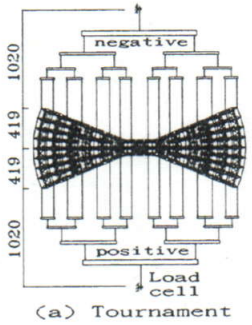

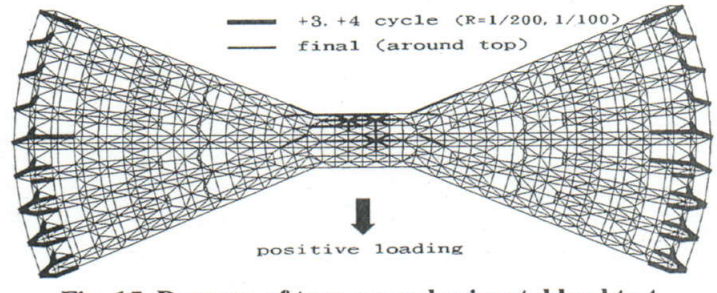

Fig. 15. Damage of transverse horizontal load test.

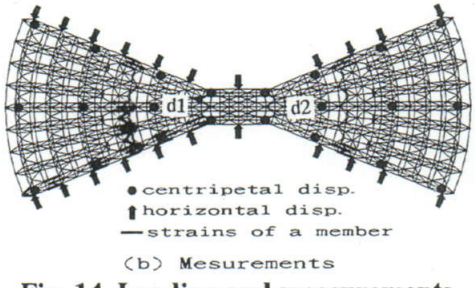

Fig. 14. Loading and measurements.

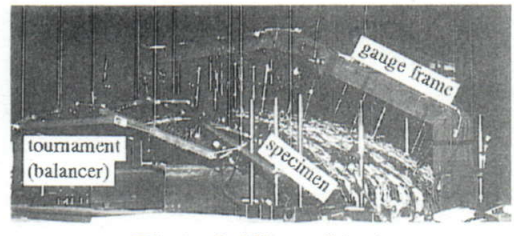

Photo 2. View of test.

solid line showing the initial shape. It is almost symmetric to the right and left. The sinking is visible and the lower parts of the front side project outward. Fig. 18 shows relations of centripetal displacements (dl and d2 in Fig. 14(b)) and horizontal displacements near the top. Sinking is accumulated by cyclic loading.

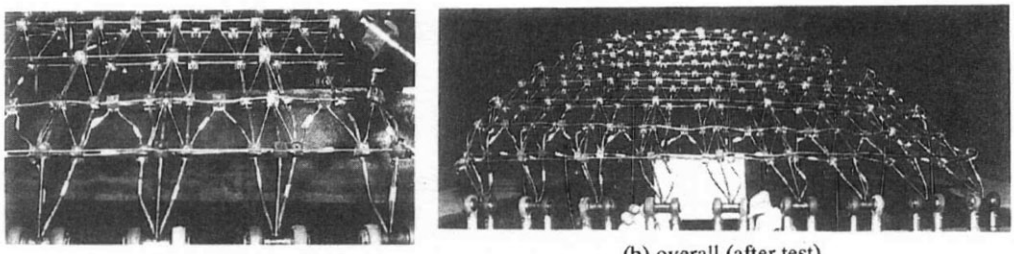

(a) around a base (−1/100 cycle)

(b) overall (after test)

Photo 3. View of damage.

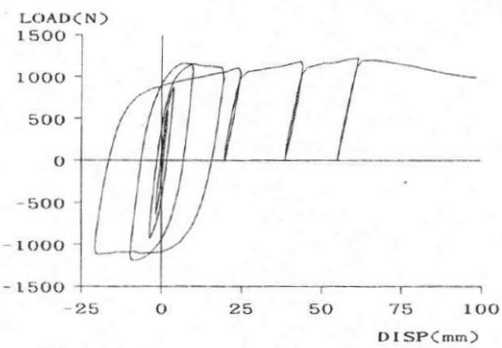

Fig. 16. Load–displacement curve.

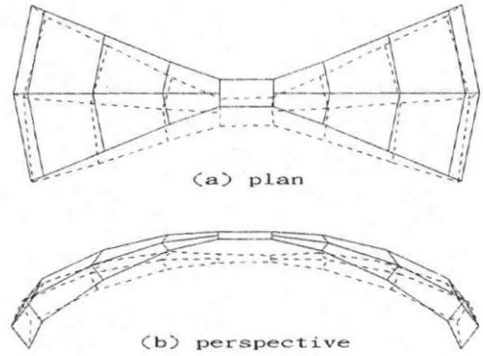

Fig. 17. Deformed shape (scale=1).

20. Macroscopic partial model. The portion above a base is modelled macroscopically as follows. Out-of-plane curvature is ignored and the X-shaped diagonals and two adjacent lower chords are replaced by one beam initially. Thus, the portion is modelled as a planar open-frame as shown in Fig. 19(a). The frame is rectangulated next and forces are considered as shown in Fig. 19(b). The bending moment of the truss-beam is also shown in the figure. It explains the reversed shear of the strain-gauged diagonals in the trussbeam-trussbeam connections.

21. Macroscopic strength. Only the calculated results are reported herein. The overall collapse mechanism strength of the partial model is 1530N, which relates to strength of secondary diagonals. On the other hand, local mechanism strength just above a base does not effect diagonal strength and is 1220N, which is almost the same as the experimental values of 1160N and 1120N. Therefore, it is considered that observed diagonal buckling hardly affects the maximum strength. In observations, chord damage was heaviest at the lower chords on bases. In

addition, the overall strength reduction after diagonal buckling is not clear and is different from that of the pyramid tests. Consequently, the experimental mechanism is considered to be macroscopic bending-yield of the main-trusses on the bases, though the first major damage is to the secondary diagonals.

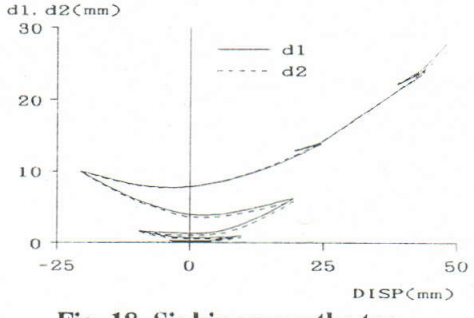

Fig. 18. Sinking near the top.

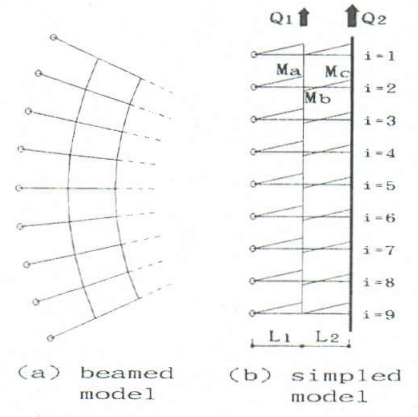

Fig. 19. Macroscopic partial model.

CONCLUSIONS

22. The following conclusions are obtained through this study. (a) A one hundredth scaled frame test is suitable and enables elasto-plastic tests for complicated complete structures. (b) Elasto-plastic member forces are calculated from experimental strains under an appropriate stress-strain model. (c) Buckling strength of chords is increased by rotational constraint from diagonals. (d) An asymmetrical vertical load test for a twin-fan-shaped specimen shows strength reduction under macroscopic instability. Strength and damaged positions in a simple planar analysis agree well with experimental results. (e) Buckling length of a chord in a rigid-jointed truss can be evaluated as that of two continuous chords, if preceded by elasto-plastic chord buckling. Ignoring rotational constraint in the case of two equal-sized chords, it is simplified as 0.7 times their nodal length. (f) A transverse horizontal load test shows diagonal buckling first and chord damage later, though the former is considered not to concern the overall collapse mechanism. Strength of the macroscopic model of the most damaged part is well matched with experimental results. (g) Macro-behaviour of a raised and double-layered space truss of complex shape may be explained by a simple model.

23. Direct comparison between design and experiment became difficult because of the copper-made specimens. This needs to be investigated analytically.

REFERENCES

1. SCHMIDT L.C., MORGAN P.R., et al. Space trusses with brittle-type strut buckling. Jour. of the Struc. Div., ASCE, 1976, vol. 102, July, 1479-1492.
2. COLLINS I.M., An investigation into the collapse behaviour of double layer grids. Proc. of the 3rd Int. Conf. on Space Struc., 1984, 400-405.
3. HORI A., et al. A structural design of a sports dome which has four retractable roofs. Annual Meeting, Arch. Inst. of Japan (AIJ), 1990, 1337-1342, (in Japanese).
4. HORI A., WADA A., et al. Static test of a model of a long-span double-layer space truss under unsymmetrical vertical load. Jour. of AIJ, 1992, June, (in Japanese).
5. HORI A., WADA A., et al. Static test of a model of a long-span double-layer space truss under transverse directional horizontal load. J. of AIJ, 1993, Feb., (in Japanese).